HHS Public Access

Author manuscript

*J Biomed Mater Res A*. Author manuscript; available in PMC 2019 June 01.

Published in final edited form as:

*J Biomed Mater Res A*. 2018 June ; 106(6): 1463–1475. doi:10.1002/jbm.a.36348.

# S-nitrosated poly(propylene sulfide) nanoparticles for enhanced nitric oxide delivery to lymphatic tissues

**Alex Schudel**[1,2], **Lauren F. Sestito**[4], and **Susan N. Thomas**[2,3,4,5,*]

[1]School of Materials Science and Engineering, Georgia Institute of Technology, 315 Ferst Dr NW, Atlanta, GA 30332, USA

[2]Parker H. Petit Institute for Bioengineering and Bioscience, Georgia Institute of Technology, 315 Ferst Dr NW, Atlanta, GA 30332, USA

[3]George W. Woodruff School of Mechanical Engineering, Georgia Institute of Technology, 315 Ferst Dr NW, Atlanta, GA 30332, USA

[4]Wallace H. Coulter Department of Biomedical Engineering, Georgia Institute of Technology, 313 Ferst Dr NW, Atlanta, GA 30332, and Emory University, 201 Dowman Drive, Atlanta, Georgia 30322

[5]Winship Cancer Institute, Emory University School of Medicine, 1365-C Clifton Road NE, Atlanta, Georgia 30322

## Abstract

Nitric oxide (NO) is a therapeutic implicated for the treatment of diseases affecting lymphatic tissues, which range from infectious and cardiovascular diseases to cancer. Existing technologies available for NO therapy, however, provide poor bioactivity within lymphatic tissues. In this work, we address this technology gap with a NO encapsulation and delivery strategy leveraging the formation of S-nitrosothiols on lymphatic-targeting Pluronic-stabilized, poly(propylene sulfide)-core nanoparticles (SNO-NP). We evaluated *in vivo* the lymphatic versus systemic delivery of NO resulting from intradermal administration of SNO-NP benchmarked against a commonly used, commercially available small molecule S-nitrosothiol NO donor, examined signs of toxicity systemically as well as localized to the site of injection, and investigated SNO effects on lymphatic transport and NP uptake by LN-resident cells. Donation of NO from SNO-NP, which scaled in proportion to the total administered dose, enhanced lymph node accumulation by two orders of magnitude without substantially reducing lymphatic transport of NP or the viability and extent of nanoparticle uptake by lymph node-resident cells. Additionally, NO delivery by SNO-NP was accompanied by low-to-negligible NO accumulation in systemic tissues with no apparent inflammation. These results suggest the utility and selectivity of SNO-NP for the targeted treatment of NO-regulated diseases that afflict lymphatic tissues.

*To whom correspondence should be addressed: Susan N. Thomas, Ph.D., George W. Woodruff School of Mechanical Engineering, Georgia Institute of Technology, 315 Ferst Drive NW, Atlanta, GA 30332, Tel: +1 (404) 385-1126, Fax: +1 (404) 385-1397, susan.thomas@gatech.edu.

**Keywords**

nanoparticle; nitric oxide; nitrosothiol; lymph nodes; lymphatics

## Introduction

The lymphatics are involved in a wide variety of diseases either as the primary tissue of interest, such as with lymphedema[1] or lymphatic filariasis,[2] or as an accessory to the pathologies of other diseases, such as with myocardial infarction[3,4] and cancer.[5] Due to the integral role lymphatics play in tissue fluid regulation,[6] lipid transport,[7] and immune cell functions,[8–10] an estimated forty million patients worldwide[11,12] endure the combined effect of all diseases in which the lymphatics are affected. Despite the high prevalence of lymphatic-associated diseases, treatment methods, especially for diseases where the lymphatics are the primary tissue of interest, remain stagnated or in some cases non-existent. As one example, the current standard for the treatment of lymphatic filariasis, an infection of lymphatic tissues by parasitic worms, is the use of antibiotic cocktails that distribute systemically to eliminate the microfilaria offspring that spread disease but do not result in appreciable drug accumulation within the lymphatics where the adult worms reside.[2] Moreover, standard therapy for lymphedema, one of the morbidities associated with both lymphatic filariasis infections and sentinel lymph node (LN) removal following breast tumor resection, employs only a combination of compression and physical therapy.[13] For diseases where the lymphatics are not the primary target but are critically involved in the disease pathology or may be useful therapeutically, such as immunotherapy[5,14–16] or LN-directed chemotherapy (e.g. for the treatment of sentinel LN metastases)[17] there exist few approved treatments that are specifically formulated to enhance delivery to lymphatics, leaving open the possibility of a range of undesired consequences including reduced treatment efficacy and toxicities related to accumulation in off target tissues.[18]

A therapeutic of particular interest for the treatment of lymphatic-related diseases is nitric oxide (NO), an extremely promiscuous signaling molecule that takes part in a variety of physiological processes ranging from vasodilation,[19–23] to neural signaling,[24] to immune cell cytotoxic defenses.[25–28] Because of the important role that NO plays in multiple physiological processess, there have been many attempts at modulating NO for therapeutic purposes. For example, NO delivered in the form of nitrate is used to control pain from angina, a disease affecting 9 million people in the US with 500,000 new cases every year, and has been found to annually cost the healthcare system around $1.9 billion.[29] NO has also been investigated in several clinical trials for use with other cardiovascular treatments to control blood pressure in adults with prehypertension,[30] which affects 25–50% of adults worldwide,[31] and to improve the function of the right of the heart following heart transplant or left ventricular assist device placement.[32] For pulmonary diseases NO is inhaled in its gaseous form, and is the current standard of care for persistent pulmonary hypertension in newborns, which affects 1.9 per 1000 live births.[33] NO has also been explored for the treatment of various cancers, including lymphoma where a variety of NO donors have been shown to be chemosensitizers[34–36] as well as exhibit direct cytotoxicity.[25,36–39]

Despite the versatility of NO as a potential therapeutic in a broad array of pathologies, several challenges exist with utilizing NO for lymphatic-related therapy. First, NO participates in many interrelated physiological processes that each have different requirements for NO signaling.[20,24,40] In some cases depletion or attenuation of NO signaling may produce negative effects such as in vascular regulation,[41] whereas in the case of inflammatory responses overproduction of NO can lead to loss of lymphatic function.[27] Consequently, a lymphatic-targeted NO-based therapy would need to be tightly controllable, since NO levels vary significantly across physiological processes and pathologies.[24,42,43] Combined with the extremely short half-life[44,45] of NO requiring it to mediate its action near its synthesis source,[44] targeted NO donation remains highly difficult. The second challenge to delivering NO, especially in the context of lymphatic-related therapies, is the result of the structure and location of the lymphatics.[10,46] To focus delivery to within the locoregional lymphatic drainage basin, direct injection in the upstream peripheral tissue interstitium is most commonly utilized,[47–49] with uptake being most favorable for macromolecular species in the range of ~10–100 nm in hydrodynamic diameter.[50,51] Since the significant majority of existing NO donors are small molecules and would thus exhibit poor selectivity for lymphatic uptake after administration in peripheral tissues,[10,46,50–52] a critical technology gap exists in facilitating NO delivery to lymphatic tissues (Figure 1a).

We previously developed[53] a NO encapsulation strategy that utilizes nanoparticles (NP) comprised of synthetic polymers that have well described profiles of lymphatic uptake[54] and biodistribution into lymphatic tissues.[55] We demonstrated that these S-nitrosated nanoparticles (SNO-NP) facilitate the controlled and sustained release of NO, enabling its cytotoxic activity against adult female *Brugia malayi* filarial worms, which are responsible for the lymphatic disease known as lymphedema.[2] Herein, we report on the preclinical testing of the NO donating activity of these SNO-NP in an *in vivo* lymphatic delivery model. We measured over the course of 72 hr the levels of various reactive nitrogen species (RNS) accumulating within systemic tissues, plasma, and LN draining the site of intradermal injection of SNO-NP and benchmarked against a commonly used, commercially available small molecule NO donor used for chemosensitization[56] and radiosensitization of cancer,[34] *S*-nitroso D,L Penicillamine (SNAP). We further assessed the impact of NO donation on lymphatic tissues by looking at lymphatic transport of NP and remodeling of the draining LN, including effects on LN-resident cells, as well as resulting inflammation at the site of injection and systemic toxicity. Our results show that donation of NO to LN when mediated by lymphatic-draining SNO-NP is dramatically improved relative to a small molecule NO donor and does not result in a measurable decrease in LN-resident cell viability or extent of NP uptake or increases in local or systemic levels of inflammation.

## Materials and Methods

### Materials

All materials were purchased from Sigma-Aldrichunless otherwise noted.

## Synthesis and Characterization of SNO-NP and SNAP

Thiolated NP were synthesized as previously described.[53] Briefly, a 0.5% solution of Pluronic F127 was made in degassed Milli-Q water. To this solution, 400 μL of propylene sulfide was added under Argon and stirred for 30 min, after which, initiator weighing 14.4, 28.8, or 43.4 mg (3.7, 7.4, and 11 mM, respectively) and reacted with 322 μL of sodium methoxide added under Argon. 1,8-diazabicyclo[5.4.0]undec-7-ene was added under Argon to the solution 15 min later and the entire reaction stirred for 24 hr. The NP solution was exposed to air for 2 hr following the reaction and dialyzed for 3 d against 4×5 L of Milli Q water using a 100,000 Da molecular weight cut off cellulose membrane dialysis tubing (Spectrum Lab). The NP were *S*-nitrosated before each experiment by reacting equal volumes of NP with sodium nitrite solution in strong acid. Unreacted free acidified nitrite was capped with addition of ammonium sulfamate and purified from the SNO-NP solution using 7 kDa Zeba columns (Thermo Fisher). SNAP solution was prepared by dissolving SNAP in 1× phosphate buffered saline (PBS) solution. S-nitrosothiol (SNO) concentrations in solutions were measured using the method of Saville (described below). For experiments that required fluorescent labeling of NP, NP were reacted with Alexa Fluor 647 $C_2$ Maleimide (Thermo Fisher) followed by excess of N-ethylmaleimide (NEM) until free thiols were no longer detectable by Ellman's assay. The solution was purified of free AlexaFluor647 and NEM using a PD-10 column (GE Healthcare). NP size was determined by dynamic light scatteringDLS (Malvern Instruments).

## IVIS Imaging

Fluorescent imaging was performed with an IVIS® Spectrum instrument (Perkin Elmer). Animals were injected intradermally in the forearm with a solution of AlexaFluor647-NP or of SNO treatment group either with or without AlexaFluor647 labeling. 24 hr later the animals were sacrified. To assess AlexaFluor647-NP drainage to LN, animals were imaged using Ex: 640, Em: 720 and an exposure of 0.1s. For the SNO-NP colocalization experiment with NO, immediately after the animals were sacrified, the skin was removed and 5 uL of a 1:1 solution of DAF-FM DA (Cayman Chemical), which works to identify NO through fluorescene due to the nitrosation of the diamino group resulting in a fluorescent triazole that has a 160-fold increase in fluroescent quantum yield and a fluorescene profile similar to fluoresceine (FITC),[57] and 1% mercuric chloride was injected into the brachial LN on the right side. The animals were then immediately imaged for both the AlexaFluor647-NP using 647 channel and DAF using the FITC channel (Ex: 500, Em: 540) at an exposure of 0.1s. Total fluorescent counts and radiant efficiency (p/s·sr·μW) were evaluated for each experiment and treatment group using elliptical regions of interest in Living Image Software (Perkin Elmer). Fluorescent signal for AlexaFluor647-NP LN drainage was normalized to the fluorescent signal measured at the site of injection.

## Use of Animals

All animal procedures were performed with IACUC approval and animals were housed in a central animal facility at Georgia Institute of Technology.

### Quantificationof NP LN accumulation

To determine the amount of NP accumulated in draining LN, either fluorescence quantification of fluorescently labelled NP[5,55] or a modified assay measuring PEG using Iodine and barium chloride, which form a barium-iodide complex of the glycol, was performed.[58,59] For the fluorescent quantifcaiton of percent of injection, LN homogenate was taken and read at 655/675 nm, and the concentration of AlexaFluor647-NP was determined using a standard curve of AlexaFluor647-NP that was allowed to react at 37°C for 24 hr. For the Iodine PEG assay centrifuged LN homogenate, BaCl solution in 1N HCL, and KI solution supplemented were reacted. The absorbance was measured at 535 nm, and the concentration of NP was determined using a standard curve of NP diluted in 1× PBS.

### Determination of SNO, $NO_2^-$, and $ONOO^-$ Concentration using Modified Saville, Griess, and Coumarin Boronic Acid (CBA) Assays

The Saville and Griess assays, which work on the principle of a two-step diazotization reaction between a sulfanilamide-based diazonium ion, formed from nitrite under acidic conditions, coupled with NEDD, were performed as previously described.[53] Briefly, sample solution (NO donor, tissue homogenate, or plasma) was mixed with either sulfanilamide solution or mercuric chloride solution prior to mixing these solutions with N-(1-Naphthyl)ethylenediamine dihydrochloride (NEDD) or 0.4N HCl. Absorbance was read at 540 nm and the difference between mercuric chloride and sulfanilamide solutions and the difference between sulfanilamide solution with and without NEDD taken as the SNO and $NO_2^-$ signals, respectively. SNO and free $NO_2^-$ concentrations were calculated using a standard curve of S-nitroso-beta-mercaptosuccinic acid. Sample peroxynitrite ($ONOO^-$) was measured using a 1:1 mixture with 100 uM Coumarin boronic acid (Cayman Chemical) (10 mg/mL in DMF diluted in 1× PBS), which works to identify ONOO- through oxidation by ONOO- to the fluorescent probe Coumarin in a stoichiometric fashion, or PBS to determine tissue background and fluorescence measured at 370/455 nm after 15 min of reaction (short time to limit possible measurement of hydrogen peroxide, which occurs at a much slower rate) $ONOO^-$ was calculated using a standard curve of $ONOO^-$ solution (Cayman Chemical) in 0.3N NaOH.

### SNO Release Studies

SNO-NP solutions in 1× PBS were incubated in closed vessels at 37°C and SNO concentrations monitored over 72 hr using the Saville assay.

### In vivo SNO LN Delivery Time Course Studies

C57BL/6J mice were injected intradermally in the forelimbs with 30 uL of treatment solution. The animals were maintained under isoflurane anesthesia for the duration of the injection. At the indicated times post injection, animals were anesthetized using isoflurance and blood harvested by cardiac puncture using a 27G needle and 1 mL syringe prefilled with 15 uL 50 mM EDTA. The blood was transferred to a microvette tube containing K4EDTA (Microvette) and stored on ice until analysis (<1 hr). Animals were then sacrificed by cervical disslocation and tissues, including LN, spleen, kidneys, and liver, were separately harvested, homogenized and weighed in preweighed tubes containing zirconium beads and

450 uL 1× PBS as previously described.[50,51] Plasma was prepared from whole blood by centrifugation at 2000 × g for 10 min, transfering the plasma layer into a microtube and retaining the supernatant. The homogenates (other than those prepared from harvested LN) were diluted to lower 5 w/w% in 1× PBS to reduce background for the Saville and Griess assays.[41,60–62] All homogenate solutions were subsequently centrifuged at 10,000 × g for 20 min and supernatants transferred for determination of SNO, $NO_2^-$, and $ONOO^-$ concentrations using the Saville, Griess, and CBA assays described above.

### Flow Cytometry

Mice were injected with SNO treatment group either with or without AlexaFluor647 labeling. 24 hr later the mice were sacrified and both LN from the same injection side of the animal were placed in 900 uL PBS on ice in the dark. 100 uL of 10 mg/mL Collagenase D solution in PBS was added to each LN well and incubated for 1 hr at 37°C. LN were then gently separated through a 70 um cell strainer into 50 mL conical tubes using a 1 mL syringe plunger. 10 mL PBS was added to push cells through and then the cells were spun down at 300 × g for 5 min. The cells were counted and then plated in their entirety into a roundbottom 96-well plate. The cells were stained with 100 uL of 2.4G2 solution, followed by Zombie Aqua Live/Dead (Biolegend) solution, and then finally monoclonal anti-mouse mAb (Biolegend) (BV411 CDllc; BV650 B220; BV711 CD3; PE CD169; AF700 CD11b). Data was acquired in a LSRFortessa (BD Biosciences) flow cytometer with compensation using either calibration beads (Thermo Fisher) or single-stained cells. Data analysis was performed using FlowJo software (FlowJo).

### Histology

2% paraformaldehyde fixed forelimbs were parrafin embedded, sliced to 10 μm thickness, decalcified, and stained with Hematoxylin and eosin. The slices were imaged using a Hamamatsu Nanozoomer.

### Statistical Analysis

Data is expressed as mean ± standard error of the mean. Statistical analysis was performed using Prism 6. Statistical significance was defined as $p \leq 0.05$.

## Results

### SNO-NP Characterization

We previously described an NO-donating NP formulation[53] based on the formation of SNO within oxidation-sensitive poly(propylene sulfide)-core, Pluronic block copolymer corona NP.[63,64] These NP are sufficiently small (~30 nm in diameter optimum for lymphatic uptake[10,46,51,54]) to be taken up into lymphatic vessels and passively transported to the draining LN[5,54,55] over the course of several days after injection (Figure 1b–c) proportional to the administered NP dose (Figure 1d).

In this NP formulation, the high concentration of free thiols in the hydrophobic NP core allows for efficient and rapid loading of NO through the formation of SNO (Figure 2a). This reaction occurs very quickly and reaches peak efficiency, as determined by the concentration

of SNO measured compared to the total NP thiol concentration, between 10–20 min of reaction time (Figure 2b). SNO formation is also most efficient when the acidified nitrite is between 2–4 equivalents of NP free thiol (Figure 2c–d), likely due to the process of nitrite converting to a nitrosating species in low pH resulting in several side reactions occurring between the acidified nitrosating species and SNO formed[65,66] that often cause the SNO decomposition. Formation of SNO-NP does not alter NP hydrodynamic size (Figure 2e), which can be synthesized to a range based on the Pluronic-to-propylene sulfide monomer ratio used,[67] nor polydispersity (data not shown), indicating that the acidic nitrosating conditions do not affect the Pluronic critical micelle concentration nor promote degradation of the stabilizing core disulfide bonds. To ensure that the loaded NO will maintain its stability in the NP over time and as dilution occurs, as well as the capacity of multiple NO doses to be utilized in a controlled manner, we tested the degradation of the SNO from SNO-NP at 37°C. SNO-NP were diluted to one of three concentrations: 10, 5, and 1 mM. SNO decay from SNO-NP was steady over the entire 72 hr for each tested dilution (Figure 2f) and the decay half-life was insensitive to starting SNO concentration (Figure 2g), indicating that as the SNO-NP concentration changes *in vivo* the release profile of SNO is not significantly altered.

## In vivo NO Donation

We next implemented a well described intradermal forearm lymphatic delivery model, whose lymphatic network efficiently drains to the ipsilateral axillary and brachial LN (Figure 1b, 3a),[5] to assess the delivery and retention of NO delivered via SNO-NP or standard small molecule SNAP. Whole animal imaging of NP and NO probe DAF-FM DA mixed 1:1 with HgCl II fluorescence 24 hr post injection revealed that only SNO-NP, which accumulated within LN draining the site of intradermal injection (Figure 3a–b), and not SNAP resulted in appreciable LN NO signal (Figure 3c–d).

Next, using the absorbance-based assays of Saville and Griess to measure RNS within harvested, homogenized tissues via endpoint analysis, we found that following intradermal administration of SNO-NP or SNAP loaded with 20 mM SNO, that SNO was only significantly elevated in the LN over the course of 72 hr post injection relative to control (PBS injected) animals when delivered via the SNO-NP (Figure 4a). These results are consistent with our image-based detection of LN-delivered NO (Figure 3) and confirm our hypothesis that small molecule NO donors are not sufficiently transported to the LN, requiring, instead, lymphatic-draining NP that can be leveraged to achieve robust SNO accumulation within the LN. Neither nitrite ($NO_2^-$) nor $ONOO^-$, RNS implicated in NO bioactivity[68] and cytotoxicity,[69,70] respectively, were detected at levels above background for any assayed time post injection with either NO donor (Figure 4b,c). As the result of SNO-NP, SNO levels in plasma were elevated 1 hr post injection, but returned to near baseline (saline) by 24 hr post injection (Figure 4d). SNAP, on the other hand, resulted in a higher but not statistically significant different plasma SNO concentration relative to saline control treated animals over the course of the experiment (Figure 4d), most likely owing to a constant clearance from the interstitial site of injection. No changes in plasma $NO_2^-$ and $ONOO^-$ levels compared to saline controls were measured over the time course of experimentation (Figure 4e–f). RNS levels in the spleen, kidneys, and liver remained

unchanged relative to saline controls over the course of the experiment for both NO donor treatment groups, except in the case of the liver where there was a small increase in $ONOO^-$ measured in animals treated with either NO donor (Figure 4h). Within dLN, however, SNO levels above those in PBS-treated animals were found to be elevated 100-fold for SNO-NP- relative to SNAP-treated animals (Figure 4g). $ONOO^-$ exposure was also modestly elevated in LN as the result of SNAP treatment (Figure 4h). Neither $NO_2^-$ nor $ONOO^-$ concentrations were elevated in plasma, whereas SNO levels increased, with SNO-NP and SNAP treatment differing ~two-fold, but not to statistically significant levels (Figure 4i).

The capacity of SNO-NP to control the level of NO delivered to lymphatic tissues was next evaluated in an *in vivo* dosing study. SNO dilutions were created via simple dilution of SNO-NP solution or when SNO-NP were formed from NP of differing thiol levels (Figure 5a). We found total dLN SNO (Figure 5b) but not $NO_2^-$ (Figure 5c) levels generated as a result of SNO-NP treatment 24 hr post injection were proportional to the concentration of total SNO administered, irrespective of how the SNO dilutions were generated. Levels of both SNO and $NO_2^-$ in plasma were either not detectable or not statistically higher than saline controls (data not shown), save the highest tested dose of SNO-NP, 20 mM. Suggesting corresponding biological effects on lymphatic tissues, LN draining the site of injection also increased in size proportionally to administered NO amount (Figure 5d); an effect attributed to the bioactive SNO since delivery of increasing concentrations of plain NP did not result in changes to the LN (data not shown).

## SNO-NP Effects on dLN-resident Cell Viability, Abundance, and NP Uptake

We next sought to begin to elucidate the effect of NO delivery to LN on resident cells. First, the viability of total (Figure 6a), $CD45^+$ (immune) cell subtypes including lymphocytes (T and B cells, CD3+B220− and B220+CD3−CD11b−, respectively), conventional and plasmacytoid dendritic cells (CDC − CD11c+B220− and PDC − CD11c+B220+, respectively), and medullary sinus, subcapsular sinus, and medullary cord macrophages (MSM − B220−CD3−CD11b+CD11c+CD169+F4/80+, SSM − B220−CD3−CD11b+CD11c+CD169+F4/80−, MCM − B220−CD3−CD11b+CD11c+CD169−F4/80+, respectively) (Figure 6b) resident cells within LN draining the site of injection 24 hr post injection was found to remain unchanged by SNO-NP treatment relative to control animals, as well as treatment with plain NP and SNAP, as assessed by flow cytometry. Despite no significant changes in viability, the abundance of cells within LN draining the site of injection was dramatically increased by SNO-NP but not SNAP or plain NP treatment; in particular T and B lymphocytes were more abundant, as well as both conventional and plasmacytoid dendritic cells and MCM subtypes, albeit for the later three cell types not to a statistically significant extent (Figure 6c). However, the proportionality of LN resident $CD45^+$ cell subpopulations remained approximately equivalent (data not shown). Notably, while the frequency of total LN-resident cells that took up or were associated with NP 24 hr post injection was somewhat reduced for SNO-NP- relative to NP-treated animals, the total number was negligibly affected by NP-mediated SNO delivery to LN (Figure 6d). SNO delivery resulted in NP associating to higher extents with CDC, PDC, and MCM (Figure 6e), and at diminished frequencies with LN-resident T and B cells (Figure 6f).

### Locoregional versus Systemic NO Donation-associated Inflammation and Toxicity

Given NO's pleiotropic and potential cytotoxic effects,[24,28,71] local and systemic markers of inflammation associated with NO donor treatment were assessed. Histological analysis of paraffin fixed slices of treated forelimbs revealed no apparent morphological changes in skin quality, thickness, or granularity for either NO donor treatment at 20 mM administered dose compared to saline control (Figure 7a). Despite increases in LN size associated with SNO-NP, but not SNAP, treatment, spleens of treated animals remained unchanged in gross size[72,73] relative to control treated animals 24 hr post injection (Figure 7b) Levels of plasma alanine transaminase and aspartate transaminase, markers of liver toxicity,[74] similarly were unchanged at all analyzed times post injection (Figure 7c).

### SNO-NP Effects on Lymphatic Transport

With evidence of SNO-NP enhancing the efficiency of SNO delivery to LN compared to small molecule NO donor SNAP, we sought to determine how changing the dose of SNO delivered would affect the overall lymphatic transport to draining LN, as NO is known to affect lymphatic pumping function.[75,76] As a metric of lymphatic transport function, total delivered amount of NP to LN was quantitatively assessed by endpoint analysis using an iodine-based absorbance assay on homogenized tissues, which overcomes the significant sensitivity limitations of whole animal imaging. NP accumulation within draining LN was sustained, with a steep increase from the time of injection to 1 to 24 hr followed by a slower and smaller increase from 24 to 72 hr (Figure 8a). Furthermore, over the range of SNO concentrations tested (6–20 mM), NP accumulation within LN draining the site of injection was only modestly diminished and in a dose-independent manner 24 hr post injection (Figure 8b).

## Discussion

While there have been several examples of reformulation of NO donors to achieve improved pharmacokinetics and biodistribution, including improving circulation time through polyethylene glycol conjugation[77] and NO bioactivity through multi-valency,[78] to our knowledge no attempts have been taken to create a NO donor specifically for targeting lymphatics.[79] Several examples exist of larger molecular weight NO donors including a 64-valency R-SNO dendrimer donor[78] and NO-containing nanoparticles;[80–84] however, all of these approaches presumably remain insufficient for NO-modulation within the lymphatics because such formulations are non-optimal for lymphatic uptake.[51]

In this work, we explored the *in vivo* NO donating capacity of a SNO-NP delivery vehicle we previously reported that exhibits controlled profiles of NO release in its bioactive form.[53] Rapidly (~10–20 min) nitrosated at close to 100% efficiency at ~2–4 molar equivalents of acidified nitrite (Figure 2b–d), these SNO-NP leverage a NP formulation, that by virtue of their size (Figure 2e) exhibit superior *in vivo* targeting of lymphatic tissues relative to conventional drug formulations (Figure 1b–d).[5,85] We found these SNO-NP, which have a SNO dose-independent half-life of 2 d, to exhibit sustained levels of accumulation within LN draining the site of intradermal injection (Figure 8b). As a result, SNO-NP significantly increase the delivered dose of SNO to LN draining the site of intradermal injection (Figure

4a), resulting in an ~100-fold increase relative to SNAP in levels of SNO exposure above PBS treated animals over 72 hr post injection (Figure 4g). This was accompanied by only an increase in plasma SNO levels 1, but not 24 or 72, hr post injection (Figure 4d), a modest (~2-fold) and not statistically significant increase in total plasma SNO exposure (Figure 4i), and no change in baseline $NO_2^-$ or $ONOO^-$ levels (Figure 4b–c,e–f,h–i). These dose-dependent effects (Figure 5), which were consistent whether generated by SNO-NP dilution of changing the extent of nitrosation through NP formulation, demonstrate the selectivity of NO, and predominantly SNO, delivery to lymphatic tissues mediated by SNO-NP is tightly controllable.

We expect much of the SNO measured over the time scales of this study to be SNO remaining on the SNO-NP due to its half-life and high starting concentration. We can also infer that SNAP, which we would expect to be cleared from the skin site of injection within minutes and to not be able to transport to the LN due to its size (~220 Da),[46,50,51] does not transnitrosate to an appreciable extent to any large molecular weight proteins such as albumin that are capable of transporting to the LN[73,86] due to the lack of increased SNO in LN draining SNAP-injected skin tissues (Figure 4a). Contrast this with increased plasma levels of SNO resulting from SNO-NP 1 hr post injection (Figure 4d). Because these 30 nm NP do not have efficient access to the blood vasculature[51,55] so would be retained for prolonged times at the site of injection[50,51] and because we have previously reported their propensity to efficiently transnitrosate physiological thiols,[53] we hypothesize that this initial spike is due to rapid transnitrosation to intradermally present small molecule thiols (cysteine for example, which can be present in excess of 100 uM[87]). Second, this may explain the only modest and dose independent changes in levels of NP LN accumulation resulting from SNO- versus plain NP (Figure 8a). Because it has been shown that attenuation of lymphatic function (characterized by an increase in diastolic diameter and a reduction in pumping frequency) occurs with application of exogenous NO,[27,86,88] it is plausible that NP accumulation within LN would be more dramatically attenuated at times post injection longer than 24 hr assessed here when more SNO has been released from SNO-NP (Figure 2f–g).

Despite the highly reactive and potentially cytotoxic nature of NO, we observed histologically no signs of inflammation at the site of SNO-NP injection, as either changes in skin thickness or granularity (Figure 7a), which is in line with several studies reporting the lack of inflammatory effects from NO donors.[82,89–95] Additionally, no increases in $ONOO^-$ were detected in any assayed tissue (Figure 4c,f,i), spleen sizes remained unchanged (Figure 7b), and plasma alanine transaminase and aspartate transaminase levels remained unchanged relative to untreated animals (Figure 7c). We did observe, however, increases in LN size (Figure 5d) that were potentially explained by flow cytometry analysis revealing dramatic increases in resident immune cell frequencies (Figure 6c), an effect potentially arising from the influx of cells circulating in the blood[96] caused by LN-delivered SNO mediated by lymphatic-draining NP. This is supported by measured frequencies of NP association with T and B cells dropping ~50% (Figure 6f) while total cell counts correspondingly increased ~30% (Figure 6c). Furthermore, the viability of LN-resident cells was not diminished by SNO-NP treatment (Figure 6a–b). Consistent with only modest decreases in total levels of NP accumulation within LN as a result of SNO co-delivery (Figure 8a), the extent of NP

uptake by LN-resident cells remained similar (Figure 6d). However, SNO-NP did associate at increased levels with dendritic cell and MCM subtypes (Figure 6e) corresponding to the measured increases in abundance of these cell subtypes (Figure 6c), while the total frequency of NP-associated cells remained similar to plain NP indicating that these cells' barrier/scavenger functions[97–99] were unperturbed by NO delivery. On the other hand, T and B cell abundance similarly increased (Figure 6c), but total frequencies of NP-associated lymphocytes were nearly inversely reduced (Figure 6f), hinting that NO release did not alter access of SNO-NP to these cells and that the reduced frequency was due to a dilution effect. Taken together, these data indicate that delivery of NO alone or in combination with co-encapsulated drug/agent to LN-resident cells in a manner roughly similar to those described for the plain (non SNO containing) NP[55] may be efficiently and rapidly achieved also by SNO-NP, while retaining the LN- and cellular biodistribution benefits of NP delivery. Of note, cellular uptake of the SNO-NP should not inhibit the function of subsequently released NO, since transnitrosation within the cell to small molecule thiols, such as cysteine, can occur and intracellular NO-species can be extracellularly released.[42,100] Therefore, NP-delivered SNO, released either extra- or intracellularly within LN, would presumably be bioactive.

In summary, we have demonstrated that SNO-NP facilitate the controlled and sustained delivery of NO to lymphatic tissues in a preclinical *in vivo* mouse model, resulting in a two order of magnitude increase in the accumulaton of SNO in the LN over the span of 72 hr post injection above control animals compared a dose-matched small molecule NO donor. Additionally, we found dramatic increases in the abundance of LN-resident lymphocytes, dendritic cells, and MCM despite no apparent LN-resident cell death associated with treament nor signs of systemic and injection site-localized toxicity after administration. Since NO has shown *in vitro/in vivo* promise with lymphatic-related cancer therapy and infectious disease applications but has been unable to progress due to delivery-related challenges, with further development this NO delivery technology has the significant potential to advance such NO-based therapeutic approaches through enhancement of lymphatic targeting.

## Acknowledgments

This work was supported by an American Heart Association Predoctoral Fellowship, the Georgia Research Alliance, National Institutes of Health grant R01CA207619, and National Institutes of Health Biomaterials Training Grant T32EB006343. We thank David M. Francis for technical assistance. The authors (except L.F.S.) have filed a patent application on the SNO-NP. Research reported in this publication was supported by the Office Of The Director, National Institutes of Health of the National Institutes of Health under Award Number S10OD016264. The content is solely the responsibility of the authors and does not necessarily represent the official views of the National Institutes of Health.

## References

1. Brandon Dixon J, Weiler MJ. Bridging the divide between pathogenesis and detection in lymphedema. Seminars in Cell & Developmental Biology. 2015; 38:75–82. [PubMed: 25545813]
2. Bockarie MJ, Taylor MJ, Gyapong JO. Current practices in the management of lymphatic filariasis. Expert Rev Anti Infect Ther. 2009; 7(5):595–605. [PubMed: 19485799]
3. Szlavy L, Adams DF, Hollenberg NK, Abrams HL. Cardiac lymph and lymphatics in normal and infarcted myocardium. American Heart Journal. 1980; 100(3):323–331. [PubMed: 7405804]

4. Szlavy L, Koster K, de Courten A, Hollenberg NK. Early disappearance of lymphatics draining ischemic myocardium in the dog. Angiology. 1987; 38(1 Pt 2):73–84. [PubMed: 3813124]
5. Thomas SN, Vokali E, Lund AW, Hubbell JA, Swartz MA. Targeting the tumor-draining lymph node with adjuvanted nanoparticles reshapes the anti-tumor immune response. Biomaterials. 2014; 35(2): 814–24. [PubMed: 24144906]
6. Swartz MA. The physiology of the lymphatic system. Advanced Drug Delivery Reviews. 2001; 50(1):3–20. [PubMed: 11489331]
7. Dixon JB. Lymphatic lipid transport: sewer or subway? Trends in Endocrinology & Metabolism. 2010; 21(8):480–487. [PubMed: 20541951]
8. Roozendaal R, Mempel TR, Pitcher LA, Gonzalez SF, Verschoor A, Mebius RE, von Andrian UH, Carroll MC. Conduits Mediate Transport of Low Molecular Weight Antigen to Lymph Node Follicles. Immunity. 2009; 30(2):264–76. [PubMed: 19185517]
9. Roozendaal R, Mebius RE, Kraal G. The conduit system of the lymph node. Int Immunol. 2008; 20(12):1483–7. [PubMed: 18824503]
10. Thomas SN, Rohner NA, Edwards EE. Implications of Lymphatic Transport to Lymph Nodes in Immunity and Immunotherapy. Annu Rev Biomed Eng. 2016; 18:207–33. [PubMed: 26928210]
11. Organization, WH. Lymphatic Filariasis Fact Sheet. 2015.
12. Organization WH. WH. News Release: Global Cancer Rates Could Increase by 50% to 15 Million by 2020. 2003
13. Didem K, Ufuk YS, Serdar S, Zumre A. The comparison of two different physiotherapy methods in treatment of lymphedema after breast surgery. Breast Cancer Res Treat. 2005; 93(1):49–54. [PubMed: 16184458]
14. Francis DM, Thomas SN. Progress and opportunities for enhancing the delivery and efficacy of checkpoint inhibitors for cancer immunotherapy. Adv Drug Deliv Rev. 2017; 114:33–42. [PubMed: 28455187]
15. Jeanbart L, Ballester M, de Titta A, Corthésy P, Romero P, Hubbell JA, Swartz MA. Enhancing Efficacy of Anticancer Vaccines by Targeted Delivery to Tumor-Draining Lymph Nodes. Cancer Immunology Research. 2014; 2(5):436–447. [PubMed: 24795356]
16. Zeng Q, Li H, Jiang H, Yu J, Wang Y, Ke H, Gong T, Zhang Z, Sun X. Tailoring polymeric hybrid micelles with lymph node targeting ability to improve the potency of cancer vaccines. Biomaterials. 2017; 122(Supplement C):105–113. [PubMed: 28110170]
17. Yang F, Jin C, Yang D, Jiang Y, Li J, Di Y, Hu J, Wang C, Ni Q, Fu D. Magnetic functionalised carbon nanotubes as drug vehicles for cancer lymph node metastasis treatment. European Journal of Cancer. 2011; 47(12):1873–1882. [PubMed: 21493061]
18. Chen SA, Sawchuk RJ, Brundage RC, Horvath C, Mendenhall HV, Gunther RA, Braeckman RA. Plasma and Lymph Pharmacokinetics of Recombinant Human Interleukin-2 and Polyethylene Glycol-Modified Interleukin-2 in Pigs. Journal of Pharmacology and Experimental Therapeutics. 2000; 293(1):248–259. [PubMed: 10734176]
19. Yao SK, Ober JC, Krishnaswami A, Ferguson JJ, Anderson HV, Golino P, Buja LM, Willerson JT. Endogenous nitric oxide protects against platelet aggregation and cyclic flow variations in stenosed and endothelium-injured arteries. Circulation. 1992; 86(4):1302–9. [PubMed: 1394936]
20. Stamler JS, Jaraki O, Osborne J, Simon DI, Keaney J, Vita J, Singel D, Valeri CR, Loscalzo J. Nitric oxide circulates in mammalian plasma primarily as an S-nitroso adduct of serum albumin. Proc Natl Acad Sci USA. 1992; 89(16):7674–7. [PubMed: 1502182]
21. Palmer RM, Ferrige AG, Moncada S. Nitric oxide release accounts for the biological activity of endothelium-derived relaxing factor. Nature. 1987; 327(6122):524–6. [PubMed: 3495737]
22. Kleschyov AL, Oelze M, Daiber A, Huang Y, Mollnau H, Schulz E, Sydow K, Fichtlscherer B, Mulsch A, Munzel T. Does nitric oxide mediate the vasodilator activity of nitroglycerin? Circ Res. 2003; 93(9):e104–12. [PubMed: 14551241]
23. Ignarro LJ, Buga GM, Wood KS, Byrns RE, Chaudhuri G. Endothelium-derived relaxing factor produced and released from artery and vein is nitric oxide. Proc Natl Acad Sci USA. 1987; 84(24): 9265–9. [PubMed: 2827174]
24. Kerwin JF Jr, Lancaster JR Jr, Feldman PL. Nitric oxide: a new paradigm for second messengers. J Med Chem. 1995; 38(22):4343–62. [PubMed: 7473563]

25. Tsumori M, Tanaka J, Koshimura K, Kawaguchi M, Murakami Y, Kato Y. Cytotoxic effect of nitric oxide on human hematological malignant cells. Acta Biochim Pol. 2002; 49(1):139–44. [PubMed: 12136934]
26. Taylor EL, Megson IL, Haslett C, Rossi AG. Nitric oxide: a key regulator of myeloid inflammatory cell apoptosis. Cell Death Differ. 2003; 10(4):418–30. [PubMed: 12719719]
27. Liao S, Cheng G, Conner DA, Huang Y, Kucherlapati RS, Munn LL, Ruddle NH, Jain RK, Fukumura D, Padera TP. Impaired lymphatic contraction associated with immunosuppression. Proceedings of the National Academy of Sciences of the United States of America. 2011; 108(46): 18784–18789. [PubMed: 22065738]
28. Laskin JD, Heck DE, Laskin DL. Multifunctional role of nitric oxide in inflammation. Trends Endocrinol Metab. 1994; 5(9):377–82. [PubMed: 18407233]
29. Boden WE, Finn AV, Patel D, Peacock WF, Thadani U, Zimmerman FH. Nitrates as an integral part of optimal medical therapy and cardiac rehabilitation for stable angina: review of current concepts and therapeutics. Clin Cardiol. 2012; 35(5):263–71. [PubMed: 22528319]
30. Schwarz, E. Study of the Effects of an Oral Nitric Oxide Supplement on Blood Pressure in Prehypertensive Adults. 2013.
31. Egan BM, Stevens-Fabry S. Prehypertension–prevalence, health risks, and management strategies. Nat Rev Cardiol. 2015; 12(5):289–300. [PubMed: 25687779]
32. Powers A. Inhaled Nitric Oxide and Inhaled Prostacyclin after Cardiac Surgery for Heart Transplant or Lvad Placement. 2012
33. Walsh-Sukys MC, Tyson JE, Wright LL, Bauer CR, Korones SB, Stevenson DK, Verter J, Stoll BJ, Lemons JA, Papile LA, others. Persistent pulmonary hypertension of the newborn in the era before nitric oxide: practice variation and outcomes. Pediatrics. 2000; 105(1 Pt 1):14–20. [PubMed: 10617698]
34. Huerta S, Chilka S, Bonavida B. Nitric oxide donors: novel cancer therapeutics (review). Int J Oncol. 2008; 33(5):909–27. [PubMed: 18949354]
35. Kim J, Yung BC, Kim WJ, Chen X. Combination of nitric oxide and drug delivery systems: tools for overcoming drug resistance in chemotherapy. J Control Release. 2017; 263:223–230. [PubMed: 28034787]
36. Huang J, Tatsumi T, Pizzoferrato E, Vujanovic N, Storkus WJ. Nitric Oxide Sensitizes Tumor Cells to Dendritic Cell–Mediated Apoptosis, Uptake, and Cross-Presentation. Cancer Research. 2005; 65(18):8461–8470. [PubMed: 16166326]
37. Umansky V, Bucur M, Schirrmacher V, Rocha M. Activated endothelial cells induce apoptosis in lymphoma cells. Int J Oncol. 1997; 10(3):465–71. [PubMed: 21533398]
38. Ushmorov A, Ratter F, Lehmann V, Droge W, Schirrmacher V, Umansky V. Nitric-oxide-induced apoptosis in human leukemic lines requires mitochondrial lipid degradation and cytochrome C release. Blood. 1999; 93(7):2342–52. [PubMed: 10090945]
39. Secchiero P, Gonelli A, Celeghini C, Mirandola P, Guidotti L, Visani G, Capitani S, Zauli G. Activation of the nitric oxide synthase pathway represents a key component of tumor necrosis factor-related apoptosis-inducing ligand-mediated cytotoxicity on hematologic malignancies. Blood. 2001; 98(7):2220–8. [PubMed: 11568010]
40. Miranda, KM., Espey, MG., Jourd'heuil, D., Grisham, MB., Fukuto, JM., Feelisch, M., Wink, DA. Louis J Nitric Oxide. San Diego: Academic Press; 2000. Chapter 3 - The Chemical Biology of Nitric Oxide A2 - Ignarro; p. 41-55.
41. Sehba FA, Schwartz AY, Chereshnev I, Bederson JB. Acute decrease in cerebral nitric oxide levels after subarachnoid hemorrhage. J Cereb Blood Flow Metab. 2000; 20(3):604–11. [PubMed: 10724124]
42. Zhang Y, Hogg N. S-Nitrosothiols: cellular formation and transport. Free Radic Biol Med. 2005; 38(7):831–8. [PubMed: 15749378]
43. Childs CE. The determination of polyethylene glycol in gamma globulin solutions. Microchemical Journal. 1975; 20(2):190–192.
44. Lancaster JR Jr, Gaston B. NO and nitrosothiols: spatial confinement and free diffusion. Am J Physiol Lung Cell Mol Physiol. 2004; 287(3):L465–6. [PubMed: 15308495]

45. Ignarro LJ. Biosynthesis and metabolism of endothelium-derived nitric oxide. Annu Rev Pharmacol Toxicol. 1990; 30:535–60. [PubMed: 2188578]
46. Thomas SN, Schudel A. Overcoming transport barriers for interstitial-, lymphatic-, and lymph node-targeted drug delivery. Curr Opin Chem Eng. 2015; 7:65–74. [PubMed: 25745594]
47. Allen TM, Hansen CB, Guo LS. Subcutaneous administration of liposomes: a comparison with the intravenous and intraperitoneal routes of injection. Biochim Biophys Acta. 1993; 1150(1):9–16. [PubMed: 8334142]
48. Kinnunen HM, Mrsny RJ. Improving the outcomes of biopharmaceutical delivery via the subcutaneous route by understanding the chemical, physical and physiological properties of the subcutaneous injection site. Journal of Controlled Release. 2014; 182(Supplement C):22–32. [PubMed: 24631859]
49. Oussoren C, Storm G. Liposomes to target the lymphatics by subcutaneous administration. Advanced Drug Delivery Reviews. 2001; 50(1):143–156. [PubMed: 11489337]
50. Rohner NA, Thomas SN. Melanoma growth effects on molecular clearance from tumors and biodistribution into systemic tissues versus draining lymph nodes. J Control Release. 2016; 223:99–108. [PubMed: 26721446]
51. Rohner NA, Thomas SN. Flexible Macromolecule versus Rigid Particle Retention in the Injected Skin and Accumulation in Draining Lymph Nodes Are Differentially Influenced by Hydrodynamic Size. ACS Biomaterials Science & Engineering. 2017; 3(2):153–159.
52. Oussoren C, Zuidema J, Crommelin DJA, Storm G. Lymphatic uptake and biodistribution of liposomes after subcutaneous injection.: II. Influence of liposomal size, lipid composition and lipid dose. Biochimica et Biophysica Acta (BBA) - Biomembranes. 1997; 1328(2):261–272. [PubMed: 9315622]
53. Schudel A, Kassis T, Dixon JB, Thomas SN. S-Nitrosated Polypropylene Sulfide Nanoparticles for Thiol-Dependent Transnitrosation and Toxicity Against Adult Female Filarial Worms. Adv Healthc Mater. 2015; 4(10):1484–90. 1423. [PubMed: 25939735]
54. Reddy ST, Berk DA, Jain RK, Swartz MA. A sensitive in vivo model for quantifying interstitial convective transport of injected macromolecules and nanoparticles. J Appl Physiol (1985). 2006; 101(4):1162–9. [PubMed: 16763103]
55. Kourtis IC, Hirosue S, de Titta A, Kontos S, Stegmann T, Hubbell JA, Swartz MA. Peripherally administered nanoparticles target monocytic myeloid cells, secondary lymphoid organs and tumors in mice. PLoS One. 2013; 8(4):e61646. [PubMed: 23626707]
56. Sullivan R, Graham CH. Chemosensitization of cancer by nitric oxide. Curr Pharm Des. 2008; 14(11):1113–23. [PubMed: 18473858]
57. Kojima H, Urano Y, Kikuchi K, Higuchi T, Hirata Y, Nagano T. Fluorescent Indicators for Imaging Nitric Oxide Production. Angew Chem Int Ed Engl. 1999; 38(21):3209–3212. [PubMed: 10556905]
58. Brown AC, Baker SR, Douglas AM, Keating M, Alvarez-Elizondo MB, Botvinick EL, Guthold M, Barker TH. Molecular interference of fibrin's divalent polymerization mechanism enables modulation of multiscale material properties. Biomaterials. 2015; 49:27–36. [PubMed: 25725552]
59. Phelps EA, Templeman KL, Thule PM, Garcia AJ. Engineered VEGF-releasing PEG-MAL hydrogel for pancreatic islet vascularization. Drug Deliv Transl Res. 2015; 5(2):125–36. [PubMed: 25787738]
60. Nahrevanian H, Dascombe MJ. Nitric oxide and reactive nitrogen intermediates during lethal and nonlethal strains of murine malaria. Parasite Immunol. 2001; 23(9):491–501. [PubMed: 11589778]
61. Mehta A, Verma RS, Srivastava N. Chlorpyrifos induced alterations in the levels of hydrogen peroxide, nitrate and nitrite in rat brain and liver. Pesticide Biochemistry and Physiology. 2009; 94(2):55–59.
62. Kostka P, Xu B, Skiles EH. Degradation of S-nitrosocysteine in vascular tissue homogenates: role of divalent ions. J Cardiovasc Pharmacol. 1999; 33(4):665–70. [PubMed: 10218740]
63. Thomas SN, Rutkowski JM, Pasquier M, Kuan EL, Alitalo K, Randolph GJ, Swartz MA. Impaired humoral immunity and tolerance in K14-VEGFR-3-Ig mice that lack dermal lymphatic drainage. J Immunol. 2012; 189(5):2181–90. [PubMed: 22844119]

64. Thomas SN, van der Vlies AJ, O'Neil CP, Reddy ST, Yu SS, Giorgio TD, Swartz MA, Hubbell JA. Engineering complement activation on polypropylene sulfide vaccine nanoparticles. Biomaterials. 2011; 32(8):2194–203. [PubMed: 21183216]

65. Hughes MN. Chemistry of nitric oxide and related species. Methods Enzymol. 2008; 436:3–19. [PubMed: 18237624]

66. Fukuto, JM., Cho, JY., Switzer, CH. Louis J Nitric Oxide. San Diego: Academic Press; 2000. Chapter 2 - The Chemical Properties of Nitric Oxide and Related Nitrogen Oxides A2 - Ignarro; p. 23-40.

67. Rehor A, Hubbell JA, Tirelli N. Oxidation-Sensitive Polymeric Nanoparticles. Langmuir. 2005; 21(1):411–417. [PubMed: 15620332]

68. Lundberg JO, Weitzberg E, Gladwin MT. The nitrate-nitrite-nitric oxide pathway in physiology and therapeutics. Nat Rev Drug Discov. 2008; 7(2):156–67. [PubMed: 18167491]

69. Radi R. Peroxynitrite, a stealthy biological oxidant. J Biol Chem. 2013; 288(37):26464–72. [PubMed: 23861390]

70. Beckman JS, Koppenol WH. Nitric oxide, superoxide, and peroxynitrite: the good, the bad, and ugly. Am J Physiol. 1996; 271(5 Pt 1):C1424–37. [PubMed: 8944624]

71. Li CQ, Pang B, Kiziltepe T, Trudel LJ, Engelward BP, Dedon PC, Wogan GN. Threshold effects of nitric oxide-induced toxicity and cellular responses in wild-type and p53-null human lymphoblastoid cells. Chem Res Toxicol. 2006; 19(3):399–406. [PubMed: 16544944]

72. Andrew PS, Deng Y, Sultanian R, Kaufman S. Nitric oxide increases fluid extravasation from the splenic circulation of the rat. Am J Physiol Regul Integr Comp Physiol. 2001; 280(4):R959–67. [PubMed: 11247815]

73. Liu H, Moynihan KD, Zheng Y, Szeto GL, Li AV, Huang B, Van Egeren DS, Park C, Irvine DJ. Structure-based Programming of Lymph Node Targeting in Molecular Vaccines. Nature. 2014; 507(7493):519–522. [PubMed: 24531764]

74. Saavedra JE, Billiar TR, Williams DL, Kim Y-M, Watkins SC, Keefer LK. Targeting Nitric Oxide (NO) Delivery in Vivo. Design of a Liver-Selective NO Donor Prodrug That Blocks Tumor Necrosis Factor-α-Induced Apoptosis and Toxicity in the Liver. Journal of Medicinal Chemistry. 1997; 40(13):1947–1954. [PubMed: 9207935]

75. Bohlen HG, Gasheva OY, Zawieja DC. Nitric oxide formation by lymphatic bulb and valves is a major regulatory component of lymphatic pumping. Am J Physiol Heart Circ Physiol. 2011; 301(5):H1897–906. [PubMed: 21890688]

76. Bohlen HG, Wang W, Gashev A, Gasheva O, Zawieja D. Phasic contractions of rat mesenteric lymphatics increase basal and phasic nitric oxide generation in vivo. Am J Physiol Heart Circ Physiol. 2009; 297(4):H1319–28. [PubMed: 19666850]

77. Katsumi H, Nishikawa M, Yamashita F, Hashida M. Development of polyethylene glycol-conjugated poly-S-nitrosated serum albumin, a novel S-Nitrosothiol for prolonged delivery of nitric oxide in the blood circulation in vivo. J Pharmacol Exp Ther. 2005; 314(3):1117–24. [PubMed: 15901798]

78. Stasko NA, Fischer TH, Schoenfisch MH. S-Nitrosothiol-Modified Dendrimers as Nitric Oxide Delivery Vehicles. Biomacromolecules. 2008; 9(3):834–841. [PubMed: 18247567]

79. Saraiva J, Samantha S Marotta-Oliveira, Simone Aparecida Cicillini, Josimar de Oliveira Eloy, Juliana Maldonado Marchetti. Nanocarriers for Nitric Oxide Delivery. Journal of Drug Delivery. 2011; 2011

80. Jo YS, van der Vlies AJ, Gantz J, Thacher TN, Antonijevic S, Cavadini S, Demurtas D, Stergiopulos N, Hubbell JA. Micelles for Delivery of Nitric Oxide. Journal of the American Chemical Society. 2009; 131(40):14413–14418. [PubMed: 19764751]

81. Seabra AB, Rai M, Durán N. Nano carriers for nitric oxide delivery and its potential applications in plant physiological process: A mini review. Journal of Plant Biochemistry and Biotechnology. 2014; 23(1):1–10.

82. Kutner AJ, Friedman AJ. Use of nitric oxide nanoparticulate platform for the treatment of skin and soft tissue infections. Wiley Interdiscip Rev Nanomed Nanobiotechnol. 2013; 5(5):502–14. [PubMed: 23661566]

83. Weller RB. Nitric Oxide–Containing Nanoparticles as an Antimicrobial Agent and Enhancer of Wound Healing. Journal of Investigative Dermatology. 2009; 129(10):2335–2337. [PubMed: 19749782]
84. Shin JH, Metzger SK, Schoenfisch MH. Synthesis of Nitric Oxide-Releasing Silica Nanoparticles. Journal of the American Chemical Society. 2007; 129(15):4612–4619. [PubMed: 17375919]
85. Kourtis, I. Therapeutic Immunomodulation of the Lymphoid-like Tumor Environment Using Nanoparticulate Formulations. 2012.
86. Weiler, M., Kassis, T., Dixon, JB. Sensitivity analysis of near-infrared functional lymphatic imaging. SPIE; 2012. p. 12
87. Braun P, Foldi M, Kisfaludy S, Szabo GY. Free Amino-acid Content of the Lymph. Nature. 1956; 177(4520):1133–1134. [PubMed: 13334501]
88. Saul ME, Thomas PA, Dosen PJ, Isbister GK, O'Leary MA, Whyte IM, McFadden SA, van Helden DF. A pharmacological approach to first aid treatment for snakebite. Nat Med. 2011; 17(7):809–11. [PubMed: 21706027]
89. Ghaffari A, Jalili R, Ghaffari M, Miller C, Ghahary A. Efficacy of gaseous nitric oxide in the treatment of skin and soft tissue infections. Wound Repair Regen. 2007; 15(3):368–77. [PubMed: 17537124]
90. Amadeu TP, Seabra AB, de Oliveira MG, Costa AM. S-nitrosoglutathione-containing hydrogel accelerates rat cutaneous wound repair. J Eur Acad Dermatol Venereol. 2007; 21(5):629–37. [PubMed: 17447976]
91. Amadeu TP, Seabra AB, de Oliveira MG, Monte-Alto-Costa A. Nitric oxide donor improves healing if applied on inflammatory and proliferative phase. J Surg Res. 2008; 149(1):84–93. [PubMed: 18374944]
92. Mowbray M, Tan X, Wheatley PS, Rossi AG, Morris RE, Weller RB. Topically applied nitric oxide induces T-lymphocyte infiltration in human skin, but minimal inflammation. J Invest Dermatol. 2008; 128(2):352–60. [PubMed: 17914444]
93. Ferrini ME, Simons BJ, Bassett DJ, Bradley MO, Roberts K, Jaffar Z. S-nitrosoglutathione reductase inhibition regulates allergen-induced lung inflammation and airway hyperreactivity. PLoS One. 2013; 8(7):e70351. [PubMed: 23936192]
94. Jia L, Pei R, Lin M, Yang X. Acute and subacute toxicity and efficacy of S-nitrosylated captopril, an ACE inhibitor possessing nitric oxide activities. Food and Chemical Toxicology. 2001; 39(12): 1135–1143. [PubMed: 11696388]
95. Gabikian P, Clatterbuck RE, Eberhart CG, Tyler BM, Tierney TS, Tamargo RJ. Prevention of experimental cerebral vasospasm by intracranial delivery of a nitric oxide donor from a controlled-release polymer: toxicity and efficacy studies in rabbits and rats. Stroke. 2002; 33(11):2681–6. [PubMed: 12411661]
96. Bellingan GJ, Caldwell H, Howie SE, Dransfield I, Haslett C. In vivo fate of the inflammatory macrophage during the resolution of inflammation: inflammatory macrophages do not die locally, but emigrate to the draining lymph nodes. The Journal of Immunology. 1996; 157(6):2577–2585. [PubMed: 8805660]
97. Sixt M, Kanazawa N, Selg M, Samson T, Roos G, Reinhardt DP, Pabst R, Lutz MB, Sorokin L. The Conduit System Transports Soluble Antigens from the Afferent Lymph to Resident Dendritic Cells in the T Cell Area of the Lymph Node. Immunity. 2005; 22(1):19–29. [PubMed: 15664156]
98. Katakai T, Hara T, Lee J-H, Gonda H, Sugai M, Shimizu A. A novel reticular stromal structure in lymph node cortex: an immuno-platform for interactions among dendritic cells, T cells and B cells. International Immunology. 2004; 16(8):1133–1142. [PubMed: 15237106]
99. Gray EE, Cyster JG. Lymph node macrophages. Journal of innate immunity. 2012; 4(5–6):424–436. [PubMed: 22488251]
100. Matsumoto A, Gow AJ. Membrane transfer of S-nitrosothiols. Nitric Oxide. 2011; 25(2):102–7. [PubMed: 21377531]

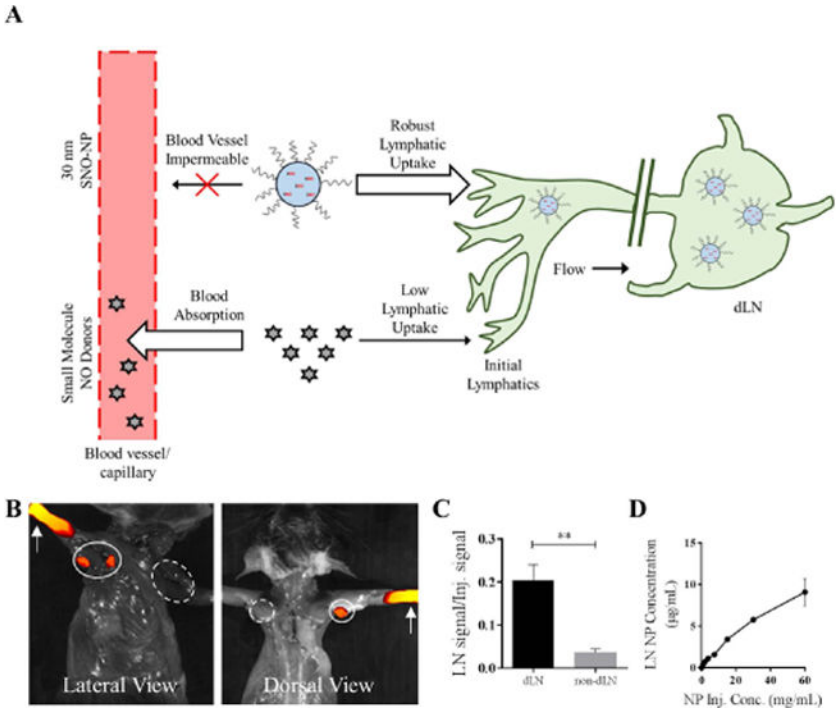


**Figure 1. Nitric oxide (NO) delivery to lymphatic tissues using lymphatic draining nanoparticles (NP)**

A) By virtue of their blood impermeability that prolongs their retention at the site of injection, hydrodynamically large drug delivery vehicles such as 30 nm lymphatic draining NP have enhanced lymphatic uptake relative to small molecules, which can be leveraged to enhance lymph node (LN) delivery of encapsulated NO. Representative IVIS images (B) and quantification (C) of AlexaFluor-647-labeled NP transport from the site of injection (white arrows) in the forearm skin to the draining ipsilateral (closed line) axillary and brachial LN (dLN) but not non-draining contralateral (dashed line) LN (non-dLN) after 24 hr. n=6 samples per group. D) NP drain to LN from the site of injection in a manner proportional to the starting concentration of injected NP. **p<0.01.

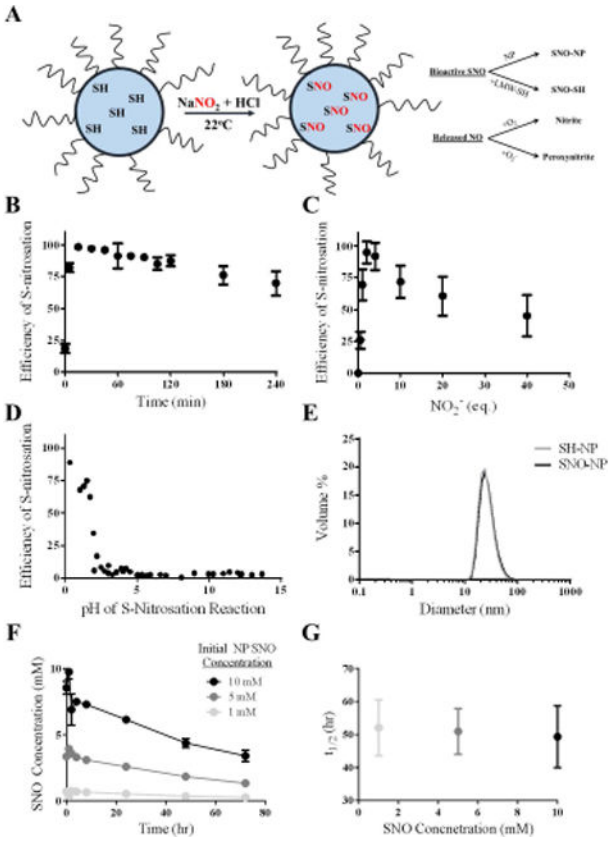


**Figure 2. Synthesis and characterization of S-nitrosothiol poly(propylene sulfide) nanoparticles (SNO-NP)**

A) Schematic of micellar structure of Pluronic-stabilized, poly(propylene sulfide) NP containing free core thiols that become S-nitrosated using an acidified sodium nitrite protocol at room temperature. SNO on the SNO-NP can either be retained on the NP or can be transnitrosated to a low molecular weight thiol (LMW-SH); NO that is released from the SNO-NP will be either oxidized with oxygen to nitrite, or will interact with superoxide and form peroxynitrite. B) Efficiency of S-nitrosation reaction, defined as the amount of S-nitrosothiol that can be generated per amount of starting free thiol concentration, reaches a maximum around 15 minutes. C) Efficiency of S-nitrosation reaches a maximum at 2–4 eq. sodium nitrite to free core thiols. D) Low pH is required for the S-nitrosation reaction with sodium nitrite and free core thiols. E) SNO-NP are stable and the same size as unmodified NP, indicating that the Pluronic-stabilized, poly(propylene sulfide) NP structure remains stable under these conditions. F) SNO decay from SNO-NP at different starting SNO concentrations over 3 d. G) The approximately 50 hour half-life of the SNO release from SNO-NP is constant at 37°C regardless of starting SNO concentration. n=3 samples per group.

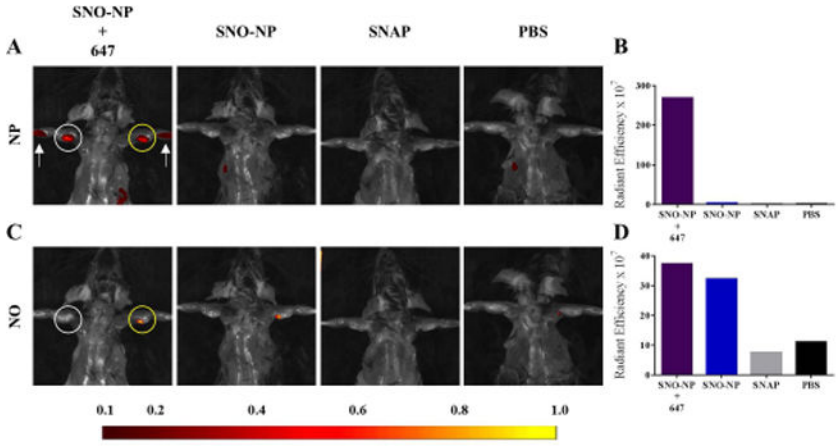


**Figure 3. Colocalization of NO and SNO-NP fluorescence in lymph nodes (LN) draining site of injection demonstrates nanoparticle-mediated lymphatic transport facilitates NO delivery to LN**

Representative IVIS images (A, C) and quantification (B, D) of AlexaFluor647 (A–B) and NO probe DAF-FM DA (C–D) fluorescence in draining LN associated with SNO-NP, but not SNAP administration in the forelimb skin. White arrow, intradermal site of treatment group injection; white circle, LN draining the site of intradermal injection; yellow circle, DAF-FM DA injected LN.

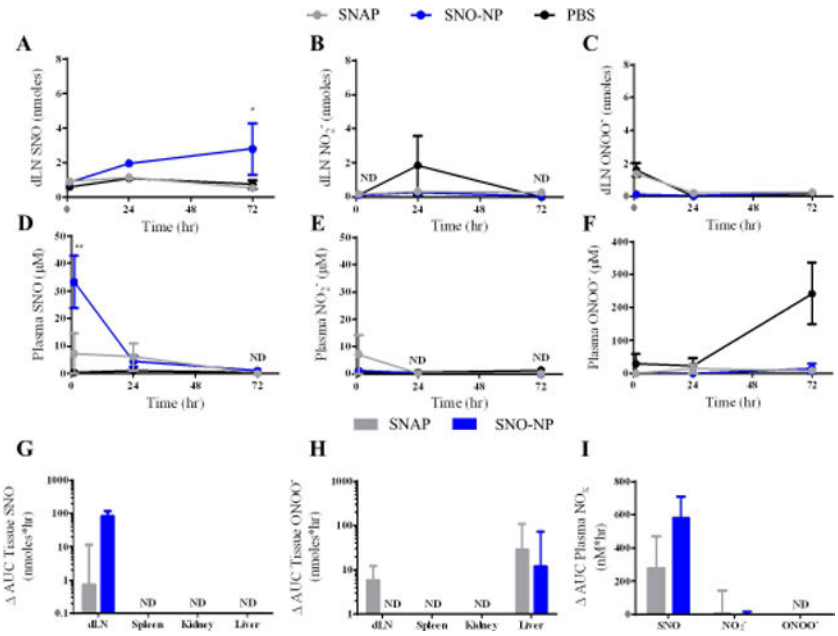


**Figure 4. SNO-NP improve delivery of SNO to lymph nodes draining the site of intradermal injection (dLN) compared to small molecule NO donor**

A) SNO-NP showed improved delivery and retention over 72 hr of SNO to lymph nodes (LN) compared to SNAP. * indicates statistically greater SNO for SNO-NP compared to SNAP. B) No appreciable accumulation of nitrite within LN for either SNO-NP or SNAP compared to control. SNO-NP and SNAP signals were not detectable (ND) at 1 or 72 hr. C) No appreciable accumulation of peroxynitrite within lymph nodes for either SNO-NP or SNAP compared to control. D) SNO-NP showed early spike in SNO concentration within plasma, whereas SNAP peaks at 24 hr. PBS and SNAP signals were ND at 72 hr. ** indicates statistically greater SNO for SNO-NP compared to SNAP. E) No appreciable accumulation of nitrite within plasma for either SNO-NP or SNAP compared to control. SNO-NP and SNAP signals were ND at 24 and 72 hr. F) No appreciable accumulation of peroxynitrite within plasma for either SNO-NP or SNAP compared to control. G) SNO-NP showed greater bias of SNO delivery compared to SNAP to LN than to plasma. Levels of SNO accumulation in the spleen, kidney, and liver were ND. H) There was a modest accumulation of peroxynitrite in the LN for SNAP but not SNO-NP, whereas in the liver there was a larger, but not statistically significant, difference in accumulation of peroxynitrite in the liver. The accumulation of peroxynitrite in the spleen and kidney was ND for all groups. I) In the plasma there was a noticeable but not statistically significant difference in the AUC of SNO signal for SNO-NP vs. SNAP. G–I, PBS AUC was subtracted from SNO-NP or SNAP AUC. For all graphs the columns/points and error bars represent the mean + SEM (n=3–6 samples per group). *$p<0.05$, **$p<0.01$.

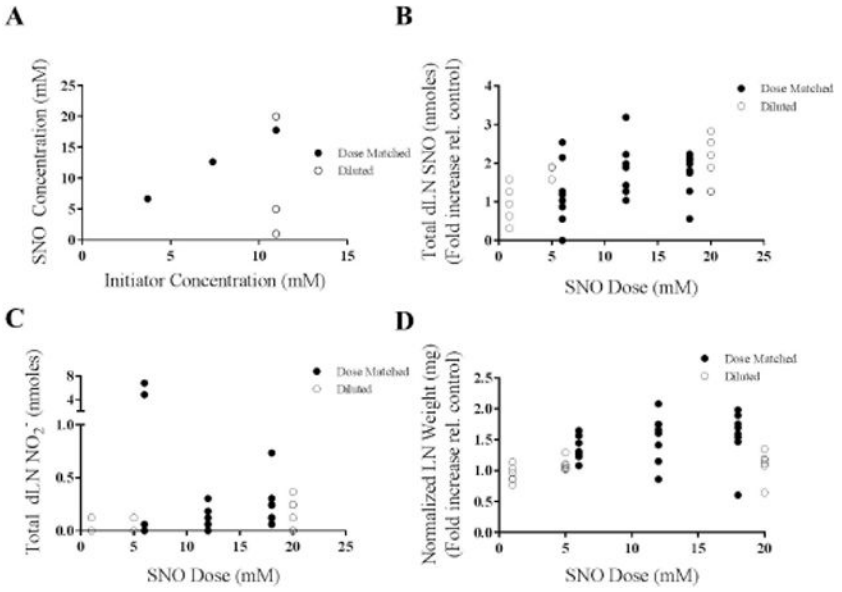


**Figure 5. SNO-NP can be synthesized to deliver a wide range of SNO doses that accumulate within the draining lymph node (dLN) in a manner proportional to concentration**

A) The SNO concentration of SNO-NP can be modified by either diluting maximally nitrosated SNO-NP with a high starting SNO concentration, or by synthesizing SNO-NP with different initiator concentrations such that the maximal nitrosation results in differing SNO concentrations due to the altered free thiol concentration. B) The total SNO within the dLN at 24 hr is proportional to the amount of SNO delivered by SNO-NP either by dilution or by dose-matched NP batches with different initiator concentrations. C) Total nitrite within the dLN at 24 hr was relatively insensitive to starting SNO concentration of SNO-NP. D) The weight of dLN 24 hr post injection was increased slightly in proportion to the starting SNO concentration of SNO-NP. For all graphs the columns/points and error bars represent the mean + SEM (n=3–8 samples per group).

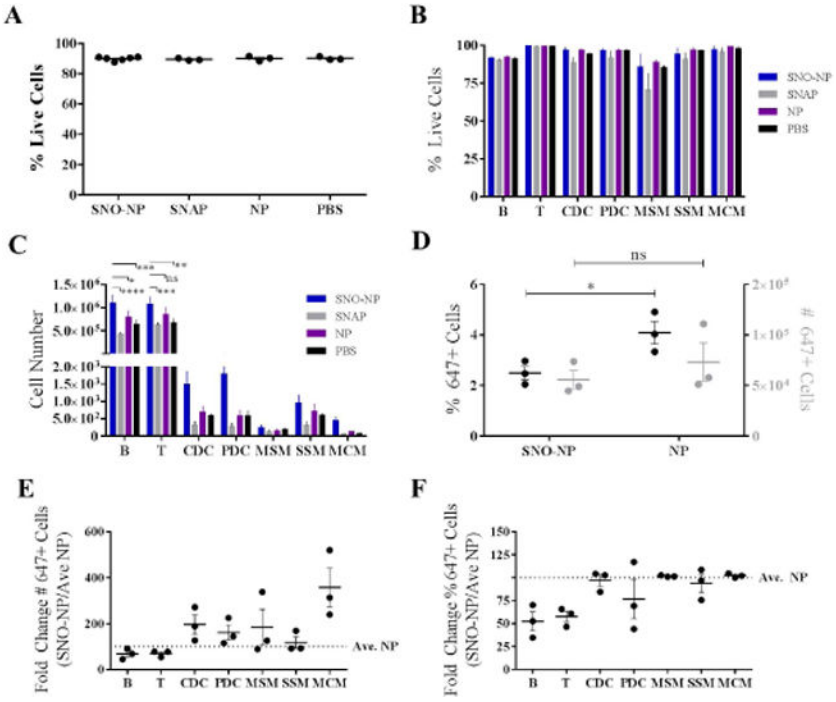


**Figure 6. SNO delivery by SNO-NP does not negatively affect the viability but increases the number of cells resident within lymph nodes draining the site of intradermal injection (dLN), resulting in modestly altered distributions of cellular NP accumulation**

A) SNO delivery from SNO-NP did not affect the viability of dLN cells compared to small molecule NO donor SNAP, plain NP, or PBS control. B) SNO delivery from SNO-NP did not alter the viability of any specific cell subtype within the LN compared to other groups. C) SNO delivery from SNO-NP resulted in increased numbers of B and T cells relative to SNAP, plain NP, and PBS control. While SNO delivery from SNO-NP also resulted in increased numbers of other cell types, the results were not statistically significant. D) SNO delivery from SNO-NP resulted in a reduction in both the number and percentage of nanoparticle positive cells. E) SNO delivered from SNO-NP resulted in an increased number of nanoparticle positive dendritic and macrophage cells while showing a slight reduction in the number of nanoparticle positive B and T cells compared to plain nanoparticle control. F) SNO delivered from SNO-NP did not affect the percentage of nanoparticle positive dendritic and macrophage cells, but did result in a drastic reduction in the percentage of nanoparticle positive B and T cells compared to plain nanoparticle control. Cells were gated as follows: B cells - B220+CD3-CD11b-; T cells – CD3+B220-; conventional dendritic cells (CDCs) – CD11c+B220-; plasmacytoid dendritic cells (PDCs) – CD11c+B220+; subcapsular sinus macrophages (SSM) – B220-CD3-CD11b+CD11c+CD169+F4/80-; medullary sinus macrophages (MSM) - B220-CD3-CD11b+CD11c+CD169+F4/80+; and medullary cord macrophages (MCM) - B220-CD3-CD11b+CD11c+CD169-F4/80+. For all graphs the columns/points and error bars represent the mean + SEM (n=3–6 samples per group). *p<0.05; **p<0.01; *** p<0.001; ****p<0.0001; ns, not significant.

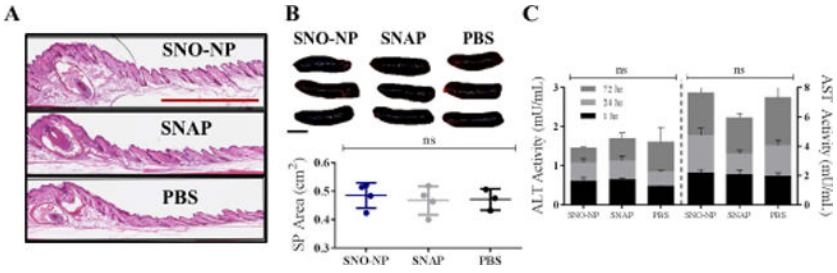


**Figure 7. Intradermal administration of SNO-NP does not result in local or systemic inflammation**

A) Representative images of the inflammation reveals no qualitative difference in skin thickness or cellularity between groups. Red bar, 1 mm. B) Top, representative spleen images from treated mice. Scale bar, 0.5 cm. Bottom, spleen sizes were found to not be statistically significantly different between groups measured after 24 hr treatment. C) There was no statistically significant difference in time-matched ALT or AST measurements from the plasma over a 72 hr time course between groups. n=3–7. ns, not significant.

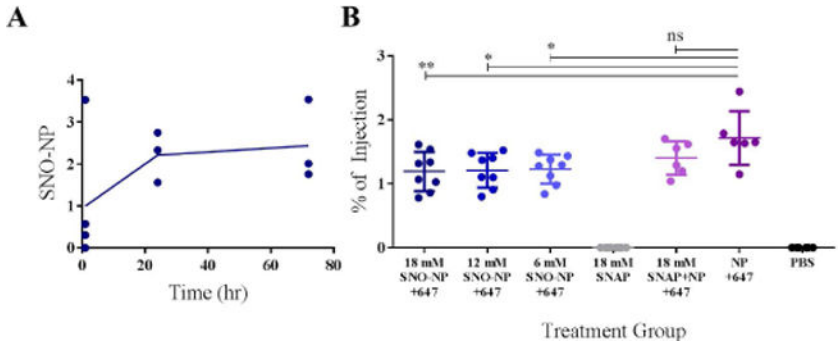


**Figure 8. SNO-NP efficiently drain to the lymph node (LN) and cause only a modest diminution in total NP LN accumulation**

A) SNO-NP drained to and accumulated in the LN over 72 hr as measured by Iodine PEG stain assay. B) There was no statistically significant difference in the percent of injection of SNO-NP solution when the dose of SNO was altered, however, compared to plain NP the presence of SNO modestly attenuated the overall accumulation of AlexaFluor647-labelled NP in LN 24 hr post injection as measured by fluorescence. For all graphs the columns/points and error bars represent the mean + SEM (n=3–8 samples per group). *$p<0.05$; **$p<0.01$; ns, not significant.